

**Glassy aerosol and  
ice nucleation**

K. J. Baustian et al.

This discussion paper is/has been under review for the journal Atmospheric Chemistry and Physics (ACP). Please refer to the corresponding final paper in ACP if available.

# State transformations and ice nucleation in glassy or (semi-)solid amorphous organic aerosol

K. J. Baustian<sup>1,2,\*</sup>, M. E. Wise<sup>1,\*\*</sup>, E. J. Jensen<sup>3</sup>, G. P. Schill<sup>1,4</sup>, M. A. Freedman<sup>5</sup>, and M. A. Tolbert<sup>4,5</sup>

<sup>1</sup>Cooperative Institute for Research in Environmental Sciences, University of Colorado, Boulder, CO, 80309, USA

<sup>2</sup>Department of Atmospheric and Oceanic Science, University of Colorado, Boulder, CO, 80309, USA

<sup>3</sup>NASA Ames Research Center, Moffett Field, CA, USA

<sup>4</sup>Department of Chemistry and Biochemistry, University of Colorado, Boulder, CO, 80309, USA

<sup>5</sup>Department of Chemistry, The Pennsylvania State University, 104 Chemistry Building, University Park, Pennsylvania 16802, USA

\* now at: School of Earth and Environment, University of Leeds, Leeds, UK

\*\* now at: College of Theology, Arts and Sciences, Concordia University, Portland, OR, 97211, USA

Title Page

Abstract

Introduction

Conclusions

References

Tables

Figures

◀

▶

◀

▶

Back

Close

Full Screen / Esc

Printer-friendly Version

Interactive Discussion



Received: 10 October 2012 – Accepted: 10 October 2012 – Published: 17 October 2012

Correspondence to: K. J. Baustian (k.baustian@leeds.ac.uk)

Published by Copernicus Publications on behalf of the European Geosciences Union.

Discussion Paper | Discussion Paper | Discussion Paper | Discussion Paper | Discussion Paper

ACPD

12, 27333–27366, 2012

## Glassy aerosol and ice nucleation

K. J. Baustian et al.

Title Page

Abstract

Introduction

Conclusions

References

Tables

Figures

⏪

⏩

◀

▶

Back

Close

Full Screen / Esc

Printer-friendly Version

Interactive Discussion



## Abstract

Glassy or amorphous (semi-)solid organic aerosol particles have the potential to serve as surfaces for heterogeneous ice nucleation in cirrus clouds. Raman spectroscopy and optical microscopy have been used in conjunction with a cold stage to examine water uptake and ice nucleation on individual aqueous organic glass particles at atmospherically relevant temperatures (200–273 K). Three organic compounds considered proxies for atmospheric secondary organic aerosol (SOA) were used in this investigation: sucrose, citric acid and glucose. Internally mixed particles consisting of each organic species and ammonium sulfate were also investigated.

Results from water uptake experiments were used to construct glass transition curves and state diagrams for each organic and corresponding mixture. A unique glass transition point on each state diagram,  $T_g'$ , was used to quantify and compare results from this study to previous works. Values of  $T_g'$  determined for aqueous sucrose, glucose and citric acid glasses were 236 K, 230 K and 220 K, respectively. Values of  $T_g'$  for internally mixed organic/sulfate particles were always significantly lower; 210 K, 207 K and 215 K for sucrose/sulfate, glucose/sulfate and citric acid/sulfate, respectively.

All investigated organic species were observed to serve as heterogeneous ice nuclei at tropospheric temperatures. Heterogeneous ice nucleation on pure organic particles occurred at  $S_{ice} = 1.1$ – $1.4$  for temperatures between 235 K and 200 K. Particles consisting of 1 : 1 organic-sulfate mixtures remained liquid over a greater range of conditions but were in some cases also observed to depositionally nucleate ice at temperatures below 202 K ( $S_{ice} = 1.25$ – $1.38$ ).

Glass transition curves constructed from experimental data were incorporated into the Community Aerosol Radiation Model for Atmospheres (CARMA) along with the predicted range of glass transition temperatures for atmospheric SOA from Koop et al. (2011). Model results suggest that organic and organic/sulfate aerosol will be glassy more than 60 % of the time in the midlatitude upper troposphere and more than 40 % of the time in the tropical tropopause region (TTL). At conditions favorable for ice

## Glassy aerosol and ice nucleation

K. J. Baustian et al.

Title Page

Abstract

Introduction

Conclusions

References

Tables

Figures

◀

▶

◀

▶

Back

Close

Full Screen / Esc

Printer-friendly Version

Interactive Discussion



formation ( $S_{ice} > 1$ ), particles in the TTL are expected to be glassy more than 50 % of the time for temperatures below 200 K. Combined with the low saturation ratios measured for ice nucleation, this work suggests heterogeneous ice formation on glassy substances may play an important role in cirrus cloud formation.

## 1 Introduction

Organic compounds are ubiquitous in tropospheric aerosol and often account for a large portion of aerosol mass (e.g. Froyd et al., 2010; Zhang et al., 2007). It has recently been proposed that oxygenated organic compounds may exist as highly viscous (semi-)solids in amorphous or glassy states at atmospherically relevant temperatures and relative humidities (RH) (Murray, 2008; Zobrist et al., 2008). The term glassy solid is used to describe an amorphous material that lacks the long-range molecular order of a crystal but behaves mechanically like a solid due to extremely high viscosity ( $> 10^{12}$  Pa s, Angell, 1995; Debenedetti and Stillinger, 2001). This transition is typically defined according to a characteristic glass transition temperature ( $T_g$ ), below which a highly viscous semi-solid is considered glassy.

The formation of glassy or amorphous (semi-)solids and their interaction with water vapor have been reviewed in the context of atmospheric aerosol by Debenedetti and Stillinger (2001), Koop et al. (2011) and Mikhailov et al. (2009). The ability of atmospheric aerosol particles to form amorphous (semi-)solids or glasses depends on aerosol composition, temperature, RH and mixing state of the particles. Zobrist et al. (2008) have shown that while many aqueous inorganic salt solutions have  $T_g$  values too low to be of importance in the atmosphere, mixtures of inorganics and oxygenated organics often have  $T_g$  values that fall within an atmospherically relevant temperature range. They suggest that glassy organic aerosol could influence water uptake and ice nucleation processes in the upper troposphere and that many atmospheric particles are glassy in state. A number of studies have provided evidence that supports this hypothesis. Koop et al. (2011) have demonstrated that typical precursors for biogenic

## Glassy aerosol and ice nucleation

K. J. Baustian et al.

Title Page

Abstract

Introduction

Conclusions

References

Tables

Figures

◀

▶

◀

▶

Back

Close

Full Screen / Esc

Printer-friendly Version

Interactive Discussion



**Glassy aerosol and ice nucleation**

K. J. Baustian et al.

Title Page

Abstract

Introduction

Conclusions

References

Tables

Figures

◀

▶

◀

▶

Back

Close

Full Screen / Esc

Printer-friendly Version

Interactive Discussion



SOA (i.e.  $\alpha$ -pinene and isoprene), when oxidized, have  $T_g$  values within the range of atmospheric relevance. Murray et al. (2012) demonstrated the solid-like behavior of iodine acid solution droplets at low RH by applying mechanical pressure. Particles shattered in a manner consistent with an ultra-viscous or glassy solid. Virtanen et al. (2010) and Saukko et al. (2012) have also inferred the solid-like behavior of SOA particles and proxies at ambient temperatures and low RHs using inertial impaction and particle bounce. Evidence that a glassy or amorphous aerosol phase influences water uptake, evaporation, diffusion, sorption and chemical aging in natural aerosol particles has also been put forth in several other recent studies (Cappa and Wilson, 2011; Roth et al., 2005; Shiraiwa et al., 2011; Vaden et al., 2011).

The present work focuses on the implications of a (semi-)solid amorphous aerosol phase for ice formation in cirrus clouds. Ice crystals form on or in ambient aerosol particles, termed ice nuclei (IN), which serve as surfaces for ice nucleation and growth in the atmosphere. Ice formation from liquid aerosol particles proceeds via a homogeneous ice nucleation pathway (Koop et al., 2000) whereas heterogeneous ice nucleation is catalyzed by a solid surface, such as an insoluble aerosol particle (Pruppacher and Klett, 1997). Particle phase will therefore determine the pathway(s) by which ice nucleation can proceed. If glassy aerosol particles are present at conditions conducive to ice formation, they could potentially serve as heterogeneous IN via the immersion, contact and depositional freezing modes. Depositional nucleation occurs when ice forms on a solid particle directly from water in the vapor phase. Immersion mode nucleation is initiated by a solid particle within an aqueous droplet whereas contact nucleation occurs when particles freeze upon touching. Cirrus clouds formed via a homogeneous mechanism will have very different properties than those formed through a heterogeneous nucleation process. Due to a low level of scientific understanding, ice cloud formation is currently not well-characterized in global models and represents a large uncertainty in predictions of climate change (Forster et al., 2007). It is therefore important that we determine whether glassy organic aerosol exists at conditions favorable for ice cloud formation, and if so, investigate ice nucleation on such particles.

**Glassy aerosol and ice nucleation**

K. J. Baustian et al.

Title Page

Abstract

Introduction

Conclusions

References

Tables

Figures

◀

▶

◀

▶

Back

Close

Full Screen / Esc

Printer-friendly Version

Interactive Discussion



There are only a few previous studies investigating ice nucleation on particles known to be glassy or (semi-)solid amorphous (Murray et al., 2010; Wagner, 2012; Wang et al., 2012a; Wilson et al., 2012). In cloud chamber experiments Murray et al. (2010) demonstrated that heterogeneous ice nucleation on glassy citric acid particles occurs at lower ice saturation ratios ( $S_{\text{ice}} = P_{\text{H}_2\text{O}}/VP_{\text{ice}}$ ) than in aqueous citric acid aerosol ( $S_{\text{ice}} \sim 1.2$  on glassy vs.  $S_{\text{ice}} \sim 1.6$  for liquid). In a follow-up study using glassy organic aerosol with a range of  $T_g$  values, Wilson et al. (2012) observed heterogeneous ice nucleation at  $S_{\text{ice}}$  values ranging from 1.2 and 1.6 for temperatures near 200 K. For the same set of experiments, Wagner et al. (2012) describes a mechanism by which initial homogeneous freezing may create a subset of amorphous aerosol particles that could then serve as highly efficient heterogeneous IN.

In the present study, we have used Raman spectroscopy and optical microscopy to investigate state transitions and ice nucleation in glassy or (semi-)solid organic aerosol particles over a range of atmospherically relevant conditions. The Raman system was used to probe phase transitions at the level of the individual particle. State diagrams constructed from experimental results were used to predict organic aerosol phase over a large range of temperatures and RH. Ice nucleation experiments were performed to determine conditions under which aqueous organic glasses can serve as heterogeneous IN. We have also incorporated laboratory results into the CARMA atmospheric model to estimate the fraction of time organic particles are likely to be glassy vs. liquid in the midlatitude upper troposphere and TTL region.

## 2 Experimental

Sucrose, glucose and citric acid are all soluble organic species known to form glassy or amorphous (semi-)solids at atmospherically relevant temperatures and RHs. These organics were chosen because they have similar functionality to soluble organic material commonly found in tropospheric aerosol particles (Graham et al., 2003) and have been

used in previous investigations of glassy or amorphous aerosol properties (Bones et al., 2012; Koop et al., 2011; Murray et al., 2010; Zobrist et al., 2008, 2011).

Tropospheric aerosol often consists of organic material internally mixed with significant fractions of inorganic compounds (e.g. Cziczo et al., 2004; Murphy et al., 2006).

Single-particle mass spectrometry has further shown that background aerosol near the TTL ( $\sim 12\text{--}18\text{ km}$ ,  $\sim 180\text{--}200\text{ K}$ ) consists mainly of internally mixed oxygenated organics and sulfates with an average organic mass fraction of 50 % (Froyd et al., 2010). For this reason, internally mixed particles containing equal parts organic and ammonium sulfate were also investigated in this study.

$T_g$  depends on both temperature and humidity. Therefore, a state diagram that shows aerosol phase as a function of both parameters is needed to predict the phase of particles in the atmosphere. A generic state diagram is shown as an example in Fig. 1. This diagram includes a melting curve ( $T_m$ , red),  $T_g$  curve (blue) and homogeneous ice nucleation curve ( $T_{\text{hom}}$ , green). These three curves define conditions under which a sample will exist in various states (glassy, liquid, metastable liquid or ice). This type of plot is referred to as a state diagram, rather than a phase diagram, because it includes both thermodynamically predicted phase transitions as well as kinetically controlled phase changes (Murray, 2008).

The two arrows shown in Fig. 1 represent experimental trajectories followed in the present study. Experiments began with glassy or amorphous (semi-)solid aerosol conditioned at low RH (pink and purple dots). RH over the sample was increased until the onset of water uptake was observed (intersection point of arrows with  $T_g$  line). Depending on the initial experimental temperature either amorphous deliquescence (pink arrow) or ice nucleation (purple arrow) was observed. Water uptake by a glassy or amorphous (semi-)solid substance generally requires higher RH at colder temperatures and is referred to as a moisture-induced phase transition or amorphous deliquescence (Mikhailov et al., 2009). If supersaturation (with respect to ice) is reached before the RH necessary for water uptake, depositional ice nucleation will be observed. The intersection point of  $T_m$  and  $T_g$  curves represents a unique point on each state diagram,

## Glassy aerosol and ice nucleation

K. J. Baustian et al.

[Title Page](#)[Abstract](#)[Introduction](#)[Conclusions](#)[References](#)[Tables](#)[Figures](#)[◀](#)[▶](#)[◀](#)[▶](#)[Back](#)[Close](#)[Full Screen / Esc](#)[Printer-friendly Version](#)[Interactive Discussion](#)

indicated as  $T_g'$  (Zobrist et al., 2008).  $T_g'$  was used in the present study to quantify and compare results from these experiments to previously published works.

## 2.1 Particle generation

Glassy or amorphous (semi-)solid particles were created by drying aqueous organic aerosol generated by atomization. Liquid aerosol particles were produced by delivering a 10 wt % solution of each organic (or 10 wt % 1 : 1 mixture with ammonium sulfate) to an atomizer (TSI 3076) at a rate of  $2 \text{ ml min}^{-1}$  using a Harvard apparatus syringe pump. Particles were impacted directly onto a silanized quartz substrate (1 mm thick) in a flow of dry  $\text{N}_2$  at  $0.6 \text{ l min}^{-1}$ . The resulting aerosol particles had diameters between 1 and  $10 \mu\text{m}$  with an average size of  $\sim 4 \mu\text{m}$ . All particles used for investigation of humidity-induced phase transitions in this study were between 3 and  $8 \mu\text{m}$  initial diameter.

Samples were placed in a experimental flow cell and exposed to an environment of dry  $\text{N}_2$  (RH  $\sim 0\%$ ,  $T = 298 \text{ K}$ ). Particles were conditioned at low RH and considered glassy or (semi-)solid amorphous, or at least to contain a glassy or semi-solid outer shell, if the following criteria were met: Raman spectra showed that particles were non-crystalline, particles were spherical and demonstrated water uptake that was not consistent with crystalline deliquescence. Spectra shown in Fig. 2 provide an example of differences between the Raman spectra of crystalline vs. glassy aqueous citric acid. Spectra from the amorphous (semi-)solid citric acid example particle lack sharp spectral features visible in the C-H ( $\sim 2900\text{--}3100 \text{ cm}^{-1}$ ) and O-H ( $\sim 3100\text{--}3600 \text{ cm}^{-1}$ ) stretching regions for the crystalline citric acid particle. Samples were held at room temperature and  $0\%$  RH until spectral subtraction showed that the water content of particles remained constant. The resulting amorphous (semi-)solid particles were never observed to effloresce, even when left for more than 24 h at RH  $\sim 0\%$ .

Crystalline samples could not be generated from atomized liquid particles due to inhibition of crystallization in concentrated organic solutions that tend to form glassy or amorphous (semi-)solids (Bodsworth et al., 2010). For experiments starting from crystalline species, a mortar and pestle was used to grind the pure crystalline material

## Glassy aerosol and ice nucleation

K. J. Baustian et al.

Title Page

Abstract

Introduction

Conclusions

References

Tables

Figures

◀

▶

◀

▶

Back

Close

Full Screen / Esc

Printer-friendly Version

Interactive Discussion



at room temperature and humidity. A small amount of the finely ground material was placed on a quartz substrate and gently tapped to free large crystals.

## 2.2 Water uptake and ice nucleation from amorphous aerosol particles

All experiments presented in this study were performed using a Raman spectrometer paired with an optical microscope, temperature-controlled environmental cell and chilled-mirror hygrometer. This experimental setup and methods have been previously described in detail by Baustian et al. (2010) and are therefore described only briefly here.

After a sample was conditioned in a dry environment at 298 K, an experiment began by introducing water vapor into the  $N_2$  stream. RH inside the cell was continuously monitored using a Buck Research CR-1A chilled-mirror hygrometer. The sample was held at 298 K until the humidity level desired for the experiment was reached and allowed to stabilize. RH was further increased by cooling the sample at a rate of  $30 \text{ K min}^{-1}$ , until the RH environment over the sample was  $\sim 90\%$  of that required for deliquescence. The sample was held at this temperature and humidity level for  $> 5$  min to ensure temperature stabilization after the initial cooling phase. A slow temperature ramp, cooling rate of  $0.1 \text{ K min}^{-1}$ , was then initiated. This rate was chosen because it is similar to the cooling rate an air parcel might experience in mid and low latitude cirrus clouds (Karcher and Strom, 2003). The sample was cooled continuously and monitored at least every 0.2 K, using both visual inspection and Raman spectroscopy, until water uptake and/or ice formation was observed. For example, if the onset of water uptake was expected to occur between 50% and 60% RH, the sample was cooled at  $30 \text{ K min}^{-1}$  until RH above the particles was  $\sim 45\%$ . After temperature equilibrium was established the sample was cooled at a rate of  $0.1 \text{ K min}^{-1}$  until the onset of water uptake was observed. Spectral subtraction was used to specifically determine RH at the onset of water uptake.

Water vapor saturation ratio with respect to ice ( $S_{\text{ice}}$ ) was also monitored and used to quantify the onset of ice nucleation events. This ratio was determined experimentally

## Glassy aerosol and ice nucleation

K. J. Baustian et al.

Title Page

Abstract

Introduction

Conclusions

References

Tables

Figures

◀

▶

◀

▶

Back

Close

Full Screen / Esc

Printer-friendly Version

Interactive Discussion



**Glassy aerosol and ice nucleation**

K. J. Baustian et al.

[Title Page](#)[Abstract](#)[Introduction](#)[Conclusions](#)[References](#)[Tables](#)[Figures](#)[I◀](#)[▶I](#)[◀](#)[▶](#)[Back](#)[Close](#)[Full Screen / Esc](#)[Printer-friendly Version](#)[Interactive Discussion](#)

from the water vapor partial pressure and the equilibrium vapor pressure of water over ice ( $S_{\text{ice}}(T) = P_{\text{H}_2\text{O}}/VP_{\text{ice}}(T)$ ).  $P_{\text{H}_2\text{O}}$  was determined from frost point values measured by the chilled-mirror hygrometer (Buck, 1981).  $VP_{\text{ice}}(T)$  was calculated using the calibrated sample temperature and vapor pressure formulations from Murphy and Koop (2005). Uncertainties in  $S_{\text{ice}}$  values listed throughout the manuscript ( $\pm 0.05$ ) reflect one standard deviation of uncertainty in the temperature calibration of the environmental cell. During experiments in which water vapor saturation with respect to ice was reached and/or surpassed, the sample was monitored for both water uptake (using Raman spectroscopy) and the onset of ice nucleation (using  $10\times$  optical magnification). For every experiment performed in this study the slow cooling phase ( $0.1 \text{ K min}^{-1}$ ) was initiated below saturation with respect to ice ( $S_{\text{ice}} < 0.9$ ). After ice nucleation was detected, the final step in every experiment was sublimation of the ice, revealing the particle responsible for nucleation. The IN was then inspected using both optical microscopy and Raman spectroscopy.

### 2.3 Experiments from pure crystalline compounds

For experiments starting from solid crystalline organic material an additional humidity cycle was needed to generate amorphous (semi-)solid particles. Crystalline samples were placed in the environmental cell at room temperature and 0% RH. Water vapor was added until the RH levels reached 90% of the deliquescence RH (DRH) of the crystalline compound and then the sample was cooled continuously at  $0.1 \text{ K min}^{-1}$  until deliquescence was observed. The resulting aqueous droplets were dried to 0% RH and warmed to 298 K to create amorphous or glassy particles. The sample was then subjected to a second humidity cycle to observe amorphous water uptake.

### 3 Results and discussion

#### 3.1 Deliquescence in crystalline vs. amorphous particles

Spectra and images obtained during a typical deliquescence experiment are shown in Fig. 2. This experiment began with a sample of crystalline citric acid monohydrate (DRH = 77 % at 298 K, Salameh et al., 2005). As RH over the sample was increased, deliquescence was observed. The left panel presents a few of the spectra and images obtained during a crystalline deliquescence experiment at 252 K. Water uptake is marked by the appearance of a broad O-H peak in the range of Raman frequencies associated with liquid water between  $\sim 3100 \text{ cm}^{-1}$  and  $\sim 3600 \text{ cm}^{-1}$ . This change is subtle due to overlapping peaks in this wavenumber range, therefore spectral subtraction was used to precisely determine onset conditions for water uptake. In this experiment crystalline deliquescence began at 76.2 % RH (Fig. 2, spectrum highlighted in blue). Deliquescence of the citric acid crystal proceeded over a small RH interval (76.2–79.5 %) as water was quickly absorbed into the bulk crystal. This transition was accompanied by dramatic changes in particle morphology as shown in the adjacent images. The newly formed liquid droplets were then dried to 0 % RH and warmed to room temperature to create concentrated amorphous (semi-)solid aerosol particles.

To demonstrate the distinct differences between crystalline and amorphous deliquescence, spectra obtained during a second humidity cycle, performed using the exact same now amorphous (semi-)solid particle, are also presented in Fig. 2 (right panel). The particle begins taking on water at much lower RH than it did during the first humidity cycle. The transition is again marked by the appearance of a peak at the characteristic Raman frequency for liquid water between  $3100 \text{ cm}^{-1}$  and  $3600 \text{ cm}^{-1}$ . The onset of water uptake in this example was observed at 30.9 % RH and indicated by the small peak around  $3400 \text{ cm}^{-1}$  (spectrum highlighted in red). In contrast to deliquescence of the crystalline particle, water uptake on the amorphous particle began at lower RH and proceeded gradually over a range of RH values as humidity was further increased. Additional spectra shown in this panel demonstrate how the particle continued to take

## Glassy aerosol and ice nucleation

K. J. Baustian et al.

Title Page

Abstract

Introduction

Conclusions

References

Tables

Figures

◀

▶

◀

▶

Back

Close

Full Screen / Esc

Printer-friendly Version

Interactive Discussion



up water over a large RH range (30.9–72.5 %, at a cooling rate of  $0.1 \text{ K min}^{-1}$ ). Optical images presented with these spectra show that hydration was not accompanied by a clear change in the size or structure of the amorphous (semi-)solid particle. Particle size did not significantly change as RH was increased up to 72.5 %. Water uptake during amorphous deliquescence can be kinetically hindered due to particle viscosity and may even be accompanied by particle shrinking due to microstructural rearrangements and the collapse of porous gel-like structures within the glassy particles (Mikhailov et al., 2009).

### 3.2 State diagrams

The left panels in Figs. 3, 4 and 5, present state diagrams constructed based on experiments with sucrose, glucose and citric acid, respectively. All square markers correspond to experiments with aqueous organic glasses whereas triangles indicate the same transition for aqueous glassy particles consisting of a 1 : 1 mixture of organic and ammonium sulfate. In all figures, open markers designate the onset of amorphous deliquescence, black markers indicate that depositional ice nucleation was observed, and gray markers indicate that both water uptake and ice nucleation took place on separate particles. In other words, gray markers denote that within the same field of view, depositional ice nucleation was observed on one particle while liquid water was observed on other particles.  $T_g(\text{RH})$  and  $T_{g\text{-mix}}(\text{RH})$  curves (red and blue) were generated by fitting polynomial equations to the experimental water uptake data for each organic. The best polynomial fits were all third order and have endpoints at the  $T_g$  of pure water (RH = 100 %,  $T_g = 136 \text{ K}$ ) at the low temperature extreme and correspond to experimentally determined  $T_g$  of each dry pure organic component (Bodsworth et al., 2010; Zobrist et al., 2008) at RH = 0 %. Fit parameters for each  $T_g(\text{RH})$  line presented in Figs. 3–5 are listed in Table A1. For clarity, the portion of each curve corresponding to experimentally determined data from the present study is shown as a solid line and the section of each curve extrapolated to endpoints is dotted. The region below (or to the

## Glassy aerosol and ice nucleation

K. J. Baustian et al.

[Title Page](#)[Abstract](#)[Introduction](#)[Conclusions](#)[References](#)[Tables](#)[Figures](#)[◀](#)[▶](#)[◀](#)[▶](#)[Back](#)[Close](#)[Full Screen / Esc](#)[Printer-friendly Version](#)[Interactive Discussion](#)

right of) the labeled  $T_g$ (RH) curves represents conditions under which aerosol particles were glassy or (semi-)solid amorphous in state. At temperatures and RH conditions above (or to the left of) the  $T_g$ (RH) curves particles took up water and were categorized as liquid aerosol. Depending on viscosity, mass transfer of water into glassy or semi-solid aerosol can be extremely slow. Above the glass transition RH, however, water uptake is a self-accelerating process and micron-sized particles tend to equilibrate with the surrounding RH environment on a timescales similar to the change in RH (10's to 100's of seconds) at ambient temperature (Tong et al., 2011). Water vapor diffusion into glassy sucrose aerosol at low temperatures is significantly slower, but enhanced by orders of magnitude at increased RH (Zobrist et al., 2011). For this reason, in the experiments detailed here, particles were considered liquid droplets once the onset of water uptake was observed.

Comparing the state diagrams constructed for each organic species, it is clear that sucrose ( $T_g' = 236$  K, Fig. 3) has the highest  $T_g'$  of the six systems investigated here. At temperatures ranging from 235 K to 270 K, sucrose particles (open squares) did not take up water until 54–71 % RH. Over the same temperature range, glucose ( $T_g' = 230$  K, Fig. 4, open squares) began taking up water at between 40–72 % RH and citric acid ( $T_g' = 220$  K, Fig. 5, open squares) from 22–68 % RH. One consequence of lower  $T_g'$  is that citric acid particles were aqueous over a wider range of conditions than the other two organic substances. Sucrose particles, on the other hand, remained in a glassy or (semi-)solid amorphous state until much higher humidity levels.

### 3.3 Comparison of $T_g$ results to other studies of laboratory-generated and ambient SOA particles

Zobrist et al. (2008) used differential scanning calorimetry to measure  $T_g$  for glucose and sucrose particles that were emulsified in oil. Despite using different techniques, our data is in good agreement for both species.  $T_g$  curves for both sucrose and glucose determined by Zobrist et al. (2008) are shifted slightly towards colder temperatures

## Glassy aerosol and ice nucleation

K. J. Baustian et al.

Title Page

Abstract

Introduction

Conclusions

References

Tables

Figures

◀

▶

◀

▶

Back

Close

Full Screen / Esc

Printer-friendly Version

Interactive Discussion



**Glassy aerosol and  
ice nucleation**

K. J. Baustian et al.

Title Page

Abstract

Introduction

Conclusions

References

Tables

Figures

◀

▶

◀

▶

Back

Close

Full Screen / Esc

Printer-friendly Version

Interactive Discussion



( $T_g'$  of 227 K and 216 K, respectively) than we have observed. However the  $T_g'$  values obtained by Zobrist et al. (2008) agree with our data to within 4 % for sucrose and 6 % for glucose. These differences are within the error bars associated with the Zobrist et al. (2008) parameterization. Zobrist et al. (2011) investigated water uptake by aqueous sucrose glasses using an electrodynamic balance. At 291 K and  $dRH/dT = 0.05 \text{ \% min}^{-1}$ , they observed a moisture-induced phase transition in micron-sized glassy sucrose particles starting at  $RH = 35 \text{ \%}$  with full transition to a liquid state by  $RH = 40 \text{ \%}$ . For higher humidity ramp rates (1 % per minute), similar to the one employed in the present study, Zobrist et al. (2011) observed the glass-to-liquid transition at 53 % RH which is in good agreement with sucrose results for presented in this manuscript.

Figure 6 shows the glass transition curves estimated by Koop et al. (2011) for a range of atmospheric SOA particles. It can be seen that our data for the pure and mixed organics fit within the Koop parameterization. Thus, the organics and mixtures used in this study are expected to be good proxies for atmospheric SOA (Wilson et al., 2012). Wang et al. (2012a) measured the onset of water uptake for laboratory proxies and ambient SOA particles using optical microscopy for detection of water uptake. For compounds with similar O : C ratio as those investigated in the present work, they found higher water uptake onset ( $\sim 15 \text{ \% RH}$  at 240 K). The difference could be due to the specific organics investigated or due to different detection methods for the onset of water uptake. However, the Wang et al. (2012a) data also fall into the Koop et al. (2011) parameterization.

### 3.4 Influence of ammonium sulfate on the $T_g(RH)$ curves of organic aerosol particles

Direct measurements of aerosol composition near the TTL region suggest the vast majority of particles consist of partially or fully neutralized sulfate mixed with oxygenated organics (Froyd et al., 2010). Froyd et al. (2010) further reported the mass fraction of organic material in the sampled background aerosol was often  $> 50 \text{ \%}$ . Thus, it is likely

that the experiments performed with organic-sulfate mixtures better represent the behavior of atmospheric particles found in the TTL.

Triangles in each state diagram show results from experiments with aerosol particles consisting of 1 : 1 internal mixtures of organic material and ammonium sulfate. In every case, the addition of ammonium sulfate shifts the  $T_g(\text{RH})$  curve of the organic substance towards colder  $T_g'$  values. This type of shift was anticipated because inorganic species tend to have lower  $T_g$  than organic species and will act as plasticizers, reducing the viscosity of a mixture compared to that of a pure compound (Koop et al., 2011; Saukko, 2012; Wilson et al., 2012; Zobrist et al., 2008). The addition of ammonium sulfate, however, does not seem to affect all of the organic substances to the same degree. For example, the ammonium sulfate has little effect on the  $T_g(\text{RH})$  of citric acid but lowers the  $T_g'$  of both sucrose and glucose by more than 20 K. In every system studied, the addition of ammonium sulfate alters the  $T_g(\text{RH})$  of each substance so that aerosol particles are liquid over a larger range of temperatures and RHs. The variable influence of ammonium sulfate on the  $T_g(\text{RH})$  of these organic compounds implies that the range of possible conditions under which organic aerosol will be glassy in the upper troposphere is highly dependent on chemical composition, particle morphology and mixing state of the aerosol.

### 3.5 Ice nucleation from aqueous organic glasses

For each system discussed above, there are certain conditions under which heterogeneous ice formation was observed. Ice formation was observed during experiments indicated by either black or gray markers on each plot of Figs. 3, 4 and 5. Black markers denote ice nucleation on glassy or (semi-)solid particles prior to water uptake, whereas gray points indicate that both water uptake and heterogeneous ice nucleation were observed simultaneously on separate particles. Onset conditions for ice nucleation are included as part of the state diagrams and the same data is also shown as a function of  $S_{\text{ice}}$  in the right panel of each figure.

## Glassy aerosol and ice nucleation

K. J. Baustian et al.

Title Page

Abstract

Introduction

Conclusions

References

Tables

Figures

◀

▶

◀

▶

Back

Close

Full Screen / Esc

Printer-friendly Version

Interactive Discussion



**Glassy aerosol and ice nucleation**

K. J. Baustian et al.

At the lowest temperatures, ice nucleation on amorphous (semi-)solid or glassy particles prior to water uptake (black markers in every figure) was typically observed. This depositional mode ice nucleation occurred with onset  $S_{\text{ice}}$  values ranging from 1.1–1.4 for temperatures of 235 K to 200 K. For experiments with aqueous sucrose glasses the average  $S_{\text{ice}}$  was  $1.19 \pm 0.08$ , which is not significantly different than the same metric for citric acid ( $S_{\text{ice, ave}} = 1.18 \pm 0.08$ ) or glucose ( $S_{\text{ice, ave}} = 1.14 \pm 0.07$ ) at temperatures below 235 K. Saturation ratios for depositional ice nucleation on these species are in excellent agreement with similar results from past studies. Results from Murray et al. (2010), who also investigated ice nucleation on glassy citric acid aerosol, are shown in Fig. 5 as black circles ( $T = 190\text{--}207$  K).

Results are also consistent with Wilson et al. (2012) who observed depositional freezing onsets between  $S_{\text{ice}} = 1.2\text{--}1.6$  ( $T < 200$  K) in cloud chamber experiments with raffinose, 4-hydroxy-3-methoxy-DL-mandelic acid, levoglucosan and a multi-component organic/sulfate mixture. Similarly, ice saturation ratios near 200 K of  $1.18 < S_{\text{ice}} < 1.57$  were reported by Schill and Tolbert (2012) for depositional nucleation on monocarboxylic films.

The results for depositional mode ice nucleation presented in this manuscript are also consistent with observations of ice nucleation on samples of laboratory and ambient SOA presumed to be glassy or amorphous (Baustian et al., 2012; Knopf et al., 2010; Wang et al., 2012a, b). Knopf et al. (2010) demonstrated that anthropogenic aerosol with a high fraction of organic material collected near Mexico City heterogeneously nucleated ice below the homogeneous freezing threshold. Wang et al. (2012b) found similar results for organic-rich aerosol samples collected in both Los Angeles and Mexico City. In the laboratory, Wang et al. (2012a) found depositional ice nucleation at  $S_{\text{ice}}$  values lower than those needed for homogeneous nucleation for naphthalene SOA proposed to be glassy.

For experiments indicated by gray markers, water uptake and ice nucleation were observed to occur simultaneously on different particles within the same field of view. For these experiments, onset of ice nucleation was observed very near the RH threshold

[Title Page](#)[Abstract](#)[Introduction](#)[Conclusions](#)[References](#)[Tables](#)[Figures](#)[◀](#)[▶](#)[◀](#)[▶](#)[Back](#)[Close](#)[Full Screen / Esc](#)[Printer-friendly Version](#)[Interactive Discussion](#)

**Glassy aerosol and ice nucleation**

K. J. Baustian et al.

Title Page

Abstract

Introduction

Conclusions

References

Tables

Figures

I◀

▶I

◀

▶

Back

Close

Full Screen / Esc

Printer-friendly Version

Interactive Discussion



for water uptake on the particles and may be explained by a competition between the water uptake and ice nucleation processes (Wang et al., 2012a).  $S_{\text{ice}}$  for the onset of ice nucleation in these experiments was always lower than  $T_{\text{hom}}$ , which rules out a homogeneous freezing pathway. Depending on whether IN particles were wet prior to ice formation, heterogeneous freezing may have occurred either by deposition or immersion modes. We are not able to determine the exact nucleation mode in this work, but the  $S_{\text{ice}}$  values obtained fit in extremely well with the deposition mode freezing data in Figs. 3, 4 and 5 (black markers). Further, the ice habit was similar to that observed in the deposition mode nucleation.

The temperature at which ice nucleation was first observed either with or without water uptake for each system was 234 K, 227 K and 220 K for sucrose, glucose and citric acid, respectively. In these experiments onset freezing temperature trended with the  $T_g$  of the dry organic compounds (Sucrose  $T_{g,\text{dry}} = 335.7$  K, Glucose  $T_{g,\text{dry}} = 296$  K; Citric Acid  $T_{g,\text{dry}} = 280$  K, Bodsworth et al., 2010; Zobrist et al., 2008) but did not strictly follow molar mass or O:C ratio of the pure organic components (Sucrose  $342.3 \text{ g mol}^{-1}$ , O:C = 0.92; Glucose  $180.16 \text{ g mol}^{-1}$ , O:C = 1.0, Citric acid  $192.124 \text{ g mol}^{-1}$ , O:C = 0.86). O:C ratios for these three organic compounds span only a small range so it is not likely to explain the large difference in onset freezing temperatures for these experiments. Wang et al. (2012a) also observed depositional ice nucleation onsets independent of O:C ratio for organic compounds with a wide range of O:C ratios.

In summary, we find that glassy aqueous organic aerosol can act as suitable surfaces for ice formation. Results indicate that heterogeneous ice nucleation proceeded at saturation ratios lower than the homogeneous nucleation threshold. The average  $S_{\text{ice}}$  for all systems studied here was  $\sim 1.2$  vs.  $S_{\text{ice}} = 1.5\text{--}1.6$  for homogeneous nucleation when  $T < 235$  K.

### 3.6 Ice nucleation on internally mixed organic-sulfate particles

Ice residues from subvisible cirrus often consist of organic/sulfate mixtures (average organic weight fraction 64 %, Froyd et al., 2010) and ice crystals are believed to form via a heterogeneous nucleation process. To help explain these observations, ice nucleation experiments were also conducted using internally mixed organic-sulfate particles. In this study, heterogeneous ice nucleation events were rarely observed on organic-sulfate particles at  $T > 200$  K.  $T_g'$  of sucrose/ammonium sulfate samples was depressed by 26 K compared to the pure organic. Mixed sucrose/ammonium sulfate particles took up water prior to ice nucleation over the entire range of temperatures investigated in this study ( $T_{g-mix}$  and open triangles, Fig. 3) and ice nucleation was never observed. For both citric acid and glucose mixed with ammonium sulfate, ice nucleation was only observed in a few experiments (gray triangles, Figs. 4 and 5) near the experimental limit of  $\sim 200$  K. The range of  $S_{ice}$  values for the onset of nucleation in these few experiments was, however, similar to those observed for the pure aqueous organic glasses. This mechanism could therefore help explain the formation of subvisible cirrus that are ever-present near the TTL ( $T \sim 180$ – $200$  K).

### 3.7 Inhibition of ammonium sulfate efflorescence in internally mixed particles

Ammonium sulfate solution droplets have been studied by many groups and efflorescence is known to occur at  $\sim 35$  % RH independent of temperature (e.g. Bodsworth et al., 2010; Martin, 2000). At low temperatures, efflorescence of ammonium sulfate may however be suppressed or eliminated in internal mixtures with high weight fractions of organic material (Bodsworth et al., 2010). During experiments in the present study, efflorescence was not observed in either organic or sulfate components of internally mixed particles. Several samples of internally mixed particles were exposed to 0 % RH for more than 24 h and crystallization was never observed. Due to the high viscosity of glassy or amorphous organic material crystallization of the ammonium sulfate was eliminated. This observation supports results from Bodsworth et al. (2010)

## Glassy aerosol and ice nucleation

K. J. Baustian et al.

Title Page

Abstract

Introduction

Conclusions

References

Tables

Figures

◀

▶

◀

▶

Back

Close

Full Screen / Esc

Printer-friendly Version

Interactive Discussion



who demonstrated that the addition of citric acid lowered the efflorescence RH, or in moderate concentrations at cold temperatures (i.e. 0.33 wt % at  $T < 250$  K), completely eliminated efflorescence in ammonium sulfate. The data presented here, also supports their conclusion that the literature efflorescence value for pure ammonium sulfate cannot always be used to predict conditions under which solid ammonium sulfate will exist in upper tropospheric aerosol.

#### 4 Atmospheric implications

Experimental results have demonstrated that glassy or ultra-viscous organic aerosol particles can serve as heterogeneous IN at tropospheric temperatures. In the atmosphere, organic aerosol will be either liquid or amorphous in phase (with a range of viscosities) depending on air parcel history and conditioning. Currently it is not known whether glassy or highly viscous aerosol particles are available for ice nucleation in the upper troposphere.

To estimate the relative importance of a mechanism for tropospheric ice cloud formation on glassy aerosol, a model was used to estimate the fraction of time glass-forming organic, mixed organic/sulfate and SOA particles would be glassy in the upper troposphere. The Community Aerosol Radiation Model for Atmospheres (CARMA) was employed following the same approach as Jensen et al. (2010). Temperature, RH,  $S_{ice}$  and aerosol phase were monitored along a large number of TTL and midlatitude air parcel trajectories. Parcel RH at the time of convective entrainment was set at 100 % with respect to liquid water. Each parcel was then monitored along its trajectory for 90 days following the point of initial injection. All particles were initially considered aqueous and remained so until parcel T and RH changed such that a glass transition would be expected. This method assumes that every particle forms a glass below  $T_g(RH)$  and that crystallization never occurs. Experimentally determined  $T_g(RH)$  curves for each species and mixture from this study were used to define particle state based on air parcel conditioning in the model. To extend results beyond the three organic species investigated

## Glassy aerosol and ice nucleation

K. J. Baustian et al.

Title Page

Abstract

Introduction

Conclusions

References

Tables

Figures

◀

▶

◀

▶

Back

Close

Full Screen / Esc

Printer-friendly Version

Interactive Discussion



in this study, the model was also run using the full range of  $T_g(\text{RH})$  values estimated for atmospheric SOA by Koop et al. (2011). Results from all model trajectories were averaged and used to estimate the fraction of time particles are expected to be glassy given conditioning in the TTL ( $185 \text{ K} < T < 220 \text{ K}$ ) and midlatitude upper tropospheric (215 K  $< T < 235 \text{ K}$ ).

Figure 7 shows the fraction of time that glass-forming aerosol particles are expected to be glassy at typical midlatitude (left) and TTL (middle) conditions. Solid colored lines in each figure correspond to results for pure organic aqueous glasses whereas colored/dashed lines indicate results for organic-sulfate mixed aerosol. Koop High, Low and Mid lines correspond to the high, low and average expected  $T_g(\text{RH})$  for atmospheric SOA from Koop et al. (2011) (depicted in Fig. 6). The fraction of time particles are predicted to be glassy for midlatitude conditions is greater than 60% for every particle type. Despite warmer temperatures in the midlatitude upper troposphere, the fraction of time particles will be glassy is overall higher compared to the TTL. This is due to generally higher RH levels found at tropical latitudes. In the TTL, every particle type is predicted to be glassy more than 40% of the time. Results for the lower TTL show greater variability because convective detrainment hydrates the air, lowering the glass fraction due to moisture-induced particle phase transitions. The glass fraction approaches 100% for all investigated scenarios at temperatures near and below 200 K. It is clear from these results that organic aerosol in both the midlatitude upper troposphere and TTL region will likely spend a significant amount of the time in a glassy or (semi-)solid amorphous state. This will, in turn, have implications on aerosol chemistry, radiative properties and CCN activity.

The same model was also used to determine whether glassy or (semi-)solid amorphous aerosol would be available to serve as heterogeneous IN at conditions conducive for ice nucleation (i.e. when  $S_{\text{ice}} > 1.0$ ). For this case, a starting point of  $S_{\text{ice}} = 1.0$  was used to set water vapor concentration and parcel RH.  $S_{\text{ice}}$  values were then tracked forward in time for each trajectory. For this type of run it was assumed that initial  $S_{\text{ice}}$  minimizes the glassy fraction because a significant portion of the aerosol

**Glassy aerosol and ice nucleation**

K. J. Baustian et al.

Title Page

Abstract

Introduction

Conclusions

References

Tables

Figures

◀

▶

◀

▶

Back

Close

Full Screen / Esc

Printer-friendly Version

Interactive Discussion



**Glassy aerosol and ice nucleation**

K. J. Baustian et al.

[Title Page](#)[Abstract](#)[Introduction](#)[Conclusions](#)[References](#)[Tables](#)[Figures](#)[◀](#)[▶](#)[◀](#)[▶](#)[Back](#)[Close](#)[Full Screen / Esc](#)[Printer-friendly Version](#)[Interactive Discussion](#)

becomes aqueous at RH levels associated with ice saturation. By sub-setting the data for  $S_{ice} > 1$ , there is generally higher RH and therefore liquid aerosol a greater fraction of time. For midlatitude “ice nucleation” trajectories (not shown here), the fraction of time aerosol was glassy remained nearly zero for all cases except pure sucrose, glucose and Koop SOA with the highest  $T_g$  temperatures. Results from the TTL “ice nucleation” scenario are shown in Fig. 7 (right). At warmer temperatures percentages ranged widely, suggesting that particle composition or  $T_g$ (RH) will strongly influence the fraction of the time it is glassy in the lower TTL. At temperatures below 200 K and  $S_{ice} > 1$ , pure organic aerosol and SOA with average to high  $T_g$  was glassy nearly 100 % of the time, independent of aerosol composition. With the exception of the glucose/sulfate particles, internally mixed particles were glassy more than 50 % of the time at 200 K. These results suggest that at conditions conducive to ice formation in the TTL particles consisting of organics, organic/sulfate mixtures or SOA are likely to be glassy or highly viscous semi-solids a large portion of the time. Therefore heterogeneous ice nucleation on glassy aerosol may provide an important mechanism for subvisible cirrus formation in the TTL.

## 5 Conclusions

In this manuscript results were presented for water uptake and depositional ice nucleation on samples of pure and internally mixed glassy or amorphous (semi-)solid aerosol particles over a wide range of atmospherically relevant conditions. Raman spectroscopy was used to construct  $T_g$ (RH) plots for aqueous sucrose, glucose, citric acid glasses and mixtures with ammonium sulfate based on moisture-induced phase transitions in the aerosol particles. Results from experiments with mixed organic-sulfate particles demonstrate the importance of aerosol mixing state for predicting partitioning between the liquid and solid amorphous phases of organic aerosol. Pure organic particles and species with higher  $T_g$  values, such as sucrose, are more likely to remain in glassy state over a larger range of atmospheric conditions.

Internally mixed organic-sulfate particles consisting of high weight fraction of (> 50%) of organic material will be liquid a larger fraction of the time compared to pure organic aerosol of the same composition. For internally mixed particles, viscous organic material was also observed to suppress efflorescence of ammonium sulfate.

Partitioning between the liquid and glassy/amorphous aerosol states will in turn dictate the pathway(s) available for ice nucleation. Results presented from the CARMA model have shown that glassy or amorphous (semi-)solid organic aerosol particles are likely present in both the midlatitude upper troposphere and TTL regions a large fraction of time. At temperatures < 200 K, such as those found in the TTL region, a pathway for heterogeneous ice formation on both organic and mixed organic-sulfate aerosol particles may also be important. When glassy aerosol is present, experimental results predict ice formation via heterogeneous nucleation at ice saturation ratios between ~ 1.2–1.4.

*Acknowledgements.* This work was supported by the National Science Foundation (ATM0650023 and AGS1048536). Also thanks to T. W. Wilson and D. J. O'Sullivan for useful discussions and advice during the preparation of this manuscript.

## References

- Angell, C. A.: Formation of Glasses From Liquids and Biopolymers, *Science*, 267, 1924–1935, doi:10.1126/science.267.5206.1924, 1995.
- Baustian, K. J., Wise, M. E., and Tolbert, M. A.: Depositional ice nucleation on solid ammonium sulfate and glutaric acid particles, *Atmos. Chem. Phys.*, 10, 2307–2317, doi:10.5194/acp-10-2307-2010, 2010.
- Baustian, K. J., Cziczo, D. J., Wise, M. E., Pratt, K. A., Kulkarni, G., Hallar, A. G., and Tolbert, M. A.: Importance of aerosol composition, mixing state, and morphology for heterogeneous ice nucleation: A combined field and laboratory approach, *J. Geophys. Res.*, 117, D06217, doi:10.1029/2011jd016784, 2012.

## Glassy aerosol and ice nucleation

K. J. Baustian et al.

Title Page

Abstract

Introduction

Conclusions

References

Tables

Figures

◀

▶

◀

▶

Back

Close

Full Screen / Esc

Printer-friendly Version

Interactive Discussion



**Glassy aerosol and ice nucleation**

K. J. Baustian et al.

[Title Page](#)[Abstract](#)[Introduction](#)[Conclusions](#)[References](#)[Tables](#)[Figures](#)[◀](#)[▶](#)[◀](#)[▶](#)[Back](#)[Close](#)[Full Screen / Esc](#)[Printer-friendly Version](#)[Interactive Discussion](#)

- Bodsworth, A., Zobrist, B., and Bertram, A. K.: Inhibition of efflorescence in mixed organic-inorganic particles at temperatures less than 250 K, *Phys. Chem. Chem. Phys.*, 12, 12259–12266, doi:10.1039/c0cp00572j, 2010.
- 5 Bones, D. L., Reid, J. P., Lienhard, D. M., and Krieger, U. K.: Comparing the mechanism of water condensation and evaporation in glassy aerosol, *P. Natl. Acad. Sci. USA*, 109, 11613–11618, doi:10.1073/pnas.1200691109, 2012.
- Buck, A. L.: New equations for computing vapor-pressure and enhancement factor, *J. Appl. Meteorol.*, 20, 1527–1532, 1981.
- 10 Cappa, C. D. and Wilson, K. R.: Evolution of organic aerosol mass spectra upon heating: implications for OA phase and partitioning behavior, *Atmos. Chem. Phys.*, 11, 1895–1911, doi:10.5194/acp-11-1895-2011, 2011.
- Cziczo, D. J., DeMott, P. J., Brooks, S. D., Prenni, A. J., Thomson, D. S., Baumgardner, D., Wilson, J. C., Kreidenweis, S. M., and Murphy, D. M.: Observations of organic species and atmospheric ice formation, *Geophys. Res. Lett.*, 31, L12116, doi:10.1029/2004gl019822, 2004.
- 15 Debenedetti, P. G. and Stillinger, F. H.: Supercooled liquids and the glass transition, *Nature*, 410, 259–267, doi:10.1038/35065704, 2001.
- Forster, P., Ramaswamy, V., Artaxo, P., Berntsen, T., Betts, R., Fahey, D. W., Haywood, J., Lean, J., Lowe, D. C., Myhre, G., Nganga, J., Prinn, R., Raga, G., Schulz, M., and Van Dorland, R.: Changes in Atmospheric Constituents and in Radiative Forcing, in: *Climate Change 2007: The Physical Science Basis. Contribution of Working Group I to the Fourth Assessment Report of the Intergovernmental Panel on Climate Change*, edited by: Solomon, S., Qin, D., Manning, M., Chen, Z., Marquis, M., Averyt, K. B., Tignor, M., and Miller, H. L., Cambridge University Press, Cambridge, 131–234, 2007.
- 20 Froyd, K. D., Murphy, D. M., Lawson, P., Baumgardner, D., and Herman, R. L.: Aerosols that form subvisible cirrus at the tropical tropopause, *Atmos. Chem. Phys.*, 10, 209–218, doi:10.5194/acp-10-209-2010, 2010.
- Graham, B., Guyon, P., Taylor, P. E., Artaxo, P., Maenhaut, W., Glovsky, M. M., Flagan, R. C., and Andreae, M. O.: Organic compounds present in the natural Amazonian aerosol: Characterization by gas chromatography-mass spectrometry, *J. Geophys. Res.-Atmos.*, 108, 4766, doi:10.1029/2003jd003990, 2003.
- 30 Jensen, E. J., Pfister, L., Bui, T.-P., Lawson, P., and Baumgardner, D.: Ice nucleation and cloud microphysical properties in tropical tropopause layer cirrus, *Atmos. Chem. Phys.*, 10, 1369–1384, doi:10.5194/acp-10-1369-2010, 2010.

**Glassy aerosol and  
ice nucleation**

K. J. Baustian et al.

[Title Page](#)[Abstract](#)[Introduction](#)[Conclusions](#)[References](#)[Tables](#)[Figures](#)[◀](#)[▶](#)[◀](#)[▶](#)[Back](#)[Close](#)[Full Screen / Esc](#)[Printer-friendly Version](#)[Interactive Discussion](#)

- Kärcher, B. and Ström, J.: The roles of dynamical variability and aerosols in cirrus cloud formation, *Atmos. Chem. Phys.*, 3, 823–838, doi:10.5194/acp-3-823-2003, 2003.
- Knopf, D. A., Wang, B., Laskin, A., Moffet, R. C., and Gilles, M. K.: Heterogeneous nucleation of ice on anthropogenic organic particles collected in Mexico City, *Geophys. Res. Lett.*, 37, L11803, doi:10.1029/2010gl043362, 2010.
- 5 Koop, T., Luo, B. P., Tsias, A., and Peter, T.: Water activity as the determinant for homogeneous ice nucleation in aqueous solutions, *Nature*, 406, 611–614, 2000.
- Koop, T., Bookhold, J., Shiraiwa, M., and Pöschl, U.: Glass transition and phase state of organic compounds: dependency on molecular properties and implications for secondary organic aerosols in the atmosphere, *Phys. Chem. Chem. Phys.*, 13, 19238–19255, 2011.
- 10 Martin, S. T.: Phase transitions of aqueous atmospheric particles, *Chem. Rev.*, 100, 3403–3453, doi:10.1021/cr990034t, 2000.
- Mikhailov, E., Vlasenko, S., Martin, S. T., Koop, T., and Pöschl, U.: Amorphous and crystalline aerosol particles interacting with water vapor: conceptual framework and experimental evidence for restructuring, phase transitions and kinetic limitations, *Atmos. Chem. Phys.*, 9, 9491–9522, doi:10.5194/acp-9-9491-2009, 2009.
- 15 Murphy, D. M. and Koop, T.: Review of the vapour pressures of ice and supercooled water for atmospheric applications, *Q. J. Roy. Meteor. Soc.*, 131, 1539–1565, doi:10.1256/qj.04.94, 2005.
- 20 Murphy, D. M., Cziczo, D. J., Froyd, K. D., Hudson, P. K., Matthew, B. M., Middlebrook, A. M., Peltier, R. E., Sullivan, A., Thomson, D. S., and Weber, R. J.: Single-particle mass spectrometry of tropospheric aerosol particles, *J. Geophys. Res.-Atmos.*, 111, D23s32, doi:10.1029/2006jd007340, 2006.
- Murray, B. J.: Inhibition of ice crystallisation in highly viscous aqueous organic acid droplets, *Atmos. Chem. Phys.*, 8, 5423–5433, doi:10.5194/acp-8-5423-2008, 2008.
- 25 Murray, B. J., Wilson, T. W., Dobbie, S., Cui, Z. Q., Al-Jumur, S., Mohler, O., Schnaiter, M., Wagner, R., Benz, S., Niemand, M., Saathoff, H., Ebert, V., Wagner, S., and Karcher, B.: Heterogeneous nucleation of ice particles on glassy aerosols under cirrus conditions, *Nat. Geosci.*, 3, 233–237, doi:10.1038/ngeo817, 2010.
- 30 Murray, B. J., Haddrell, A. E., Peppe, S., Davies, J. F., Reid, J. P., O'Sullivan, D., Price, H. C., Kumar, R., Saunders, R. W., Plane, J. M. C., Umo, N. S., and Wilson, T. W.: Glass formation and unusual hygroscopic growth of iodine acid solution droplets with relevance for iodine me-

**Glassy aerosol and ice nucleation**

K. J. Baustian et al.

Title Page

Abstract

Introduction

Conclusions

References

Tables

Figures

◀

▶

◀

▶

Back

Close

Full Screen / Esc

Printer-friendly Version

Interactive Discussion



diated particle formation in the marine boundary layer, *Atmos. Chem. Phys.*, 12, 8575–8587, doi:10.5194/acp-12-8575-2012, 2012.

Pruppacher, H. R. and Klett, J. D.: *Microphysics of Clouds and Precipitation*, edited by: Reidel, D., Norwell, Mass., 1997.

5 Roth, C. M., Goss, K. U., and Schwarzenbach, R. P.: Sorption of a diverse set of organic vapors to urban aerosols, *Environ. Sci. Technol.*, 39, 6638–6643, doi:10.1021/es0503837, 2005.

Salameh, A. K., Mauer, A. K., and Taylor, L. S.: Implications of Deliquescence in Food and Pharmaceutical Products Ninth Topical Conference on Food Engineering (CoFE 2005) Cincinnati, OH, USA, 2 November 2005, 2005.

10 Saukko, E., Lambe, A. T., Massoli, P., Koop, T., Wright, J. P., Croasdale, D. R., Pedernera, D. A., Onasch, T. B., Laaksonen, A., Davidovits, P., Worsnop, D. R., and Virtanen, A.: Humidity-dependent phase state of SOA particles from biogenic and anthropogenic precursors, *Atmos. Chem. Phys.*, 12, 7517–7529, doi:10.5194/acp-12-7517-2012, 2012.

Schill, G. P. and Tolbert, M. A.: Depositional Ice Nucleation on Monocarboxylic Acids: Effect of the O:C Ratio, *J. Phys. Chem. A*, 116, 6817–6822, doi:10.1021/jp301772q, 2012.

15 Shiraiwa, M., Ammann, M., Koop, T., and Pöschl, U.: Gas uptake and chemical aging of semisolid organic aerosol particles, *P. Natl. Acad. Sci. USA*, 108, 11003–11008, doi:10.1073/pnas.1103045108, 2011.

Tong, H.-J., Reid, J. P., Bones, D. L., Luo, B. P., and Krieger, U. K.: Measurements of the timescales for the mass transfer of water in glassy aerosol at low relative humidity and ambient temperature, *Atmos. Chem. Phys.*, 11, 4739–4754, doi:10.5194/acp-11-4739-2011, 2011.

Vaden, T. D., Imre, D., Beranek, J., Shrivastava, M., and Zelenyuk, A.: Evaporation kinetics and phase of laboratory and ambient secondary organic aerosol, *P. Natl. Acad. Sci. USA*, 108, 2190–2195, doi:10.1073/pnas.1013391108, 2011.

25 Virtanen, A., Joutsensaari, J., Koop, T., Kannosto, J., Yli-Pirila, P., Leskinen, J., Makela, J. M., Holopainen, J. K., Pöschl, U., Kulmala, M., Worsnop, D. R., and Laaksonen, A.: An amorphous solid state of biogenic secondary organic aerosol particles, *Nature*, 467, 824–827, doi:10.1038/nature09455, 2010.

30 Wagner, R., Möhler, O., Saathoff, H., Schnaiter, M., Skrotzki, J., Leisner, T., Wilson, T. W., Malkin, T. L., and Murray, B. J.: Ice cloud processing of ultra-viscous/glassy aerosol particles leads to enhanced ice nucleation ability, *Atmos. Chem. Phys.*, 12, 8589–8610, doi:10.5194/acp-12-8589-2012, 2012.

**Glassy aerosol and ice nucleation**

K. J. Baustian et al.

- Wang, B., Lambe, A. T., Massoli, P., Onasch, T. B., Davidovits, P., Worsnop, D. R., and Knopf, D. A.: The deposition ice nucleation and immersion freezing potential of amorphous secondary organic aerosol: pathways for ice and mixed-phase cloud formation, *J. Geophys. Res.*, 117, D16209, doi:10.1029/2012jd018063, 2012a.
- 5 Wang, B., Laskin, A., Roedel, T., Gilles, M. K., Moffet, R. C., Tivanski, A., and Knopf, D. A.: Heterogeneous ice nucleation and water uptake by field-collected atmospheric particles below 273 K, *J. Geophys. Res.*, 117, D00V19, doi:10.1029/2012JD017446, 2012b.
- Wilson, T. W., Murray, B. J., Wagner, R., Möhler, O., Saathoff, H., Schnaiter, M., Skrotzki, J., Price, H. C., Malkin, T. L., Dobbie, S., and Al-Jumur, S. M. R. K.: Glassy aerosols with a  
10 range of compositions nucleate ice heterogeneously at cirrus temperatures, *Atmos. Chem. Phys.*, 12, 8611–8632, doi:10.5194/acp-12-8611-2012, 2012.
- Zhang, Q., Jimenez, J. L., Canagaratna, M. R., Allan, J. D., Coe, H., Ulbrich, I., Alfarra, M. R., Takami, A., Middlebrook, A. M., Sun, Y. L., Dzepina, K., Dunlea, E., Docherty, K., DeCarlo, P. F., Salcedo, D., Onasch, T., Jayne, J. T., Miyoshi, T., Shimonono, A., Hatakeyama, S., Takegawa, N., Kondo, Y., Schneider, J., Drewnick, F., Borrmann, S., Weimer, S., Demerjian, K., Williams, P., Bower, K., Bahreini, R., Cottrell, L., Griffin, R. J., Rautiainen, J., Sun, J. Y., Zhang, Y. M., and Worsnop, D. R.: Ubiquity and dominance of oxygenated species in organic aerosols in anthropogenically-influenced Northern Hemisphere midlatitudes, *Geophys. Res. Lett.*, 34, L13801, doi:10.1029/2007gl029979, 2007.
- 15 Zobrist, B., Marcolli, C., Pedernera, D. A., and Koop, T.: Do atmospheric aerosols form glasses?, *Atmos. Chem. Phys.*, 8, 5221–5244, doi:10.5194/acp-8-5221-2008, 2008.
- Zobrist, B., Soonsin, V., Luo, B. P., Krieger, U. K., Marcolli, C., Peter, T., and Koop, T.: Ultra-slow water diffusion in aqueous sucrose glasses, *Phys. Chem. Chem. Phys.*, 13, 3514–3526, doi:10.1039/c0cp01273d, 2011.
- 20

[Title Page](#)[Abstract](#)[Introduction](#)[Conclusions](#)[References](#)[Tables](#)[Figures](#)[◀](#)[▶](#)[◀](#)[▶](#)[Back](#)[Close](#)[Full Screen / Esc](#)[Printer-friendly Version](#)[Interactive Discussion](#)

## Glassy aerosol and ice nucleation

K. J. Baustian et al.

**Table A1.** Fit parameters for  $T_g(\text{RH})$  lines for all investigated aqueous organic glasses and mixtures.  $Y = A + BX + CX^2$  where  $X$  is humidity from 0–100% and  $Y$  is temperature in Kelvin. Parameters are listed along with uncertainties at the one standard deviation level.

Substance	$a$	$b$	$c$	$R^2$
Sucrose	$333.94 \pm 4.89$	$-0.30 \pm 0.18$	$-0.017 \pm 0.0017$	0.99
Sucrose/AS	$278.53 \pm 5.47$	$-0.99 \pm 0.23$	$-0.0037 \pm 0.0021$	0.98
Glucose	$293.26 \pm 5.61$	$0.12 \pm 0.19$	$-0.016 \pm 0.0019$	0.97
Glucose/AS	$288.91 \pm 4.01$	$-1.39 \pm 0.15$	$-0.0013 \pm 0.0013$	0.99
Citric Acid	$277.14 \pm 4.66$	$-0.33 \pm 0.18$	$-0.010 \pm 0.0018$	0.97
Citric Acid/AS	$282.59 \pm 8.99$	$-0.75 \pm 0.33$	$-0.0066 \pm 0.0028$	0.97

[Title Page](#)
[Abstract](#)
[Introduction](#)
[Conclusions](#)
[References](#)
[Tables](#)
[Figures](#)
[I◀](#)
[▶I](#)
[◀](#)
[▶](#)
[Back](#)
[Close](#)
[Full Screen / Esc](#)
[Printer-friendly Version](#)
[Interactive Discussion](#)


**Glassy aerosol and  
ice nucleation**

K. J. Baustian et al.

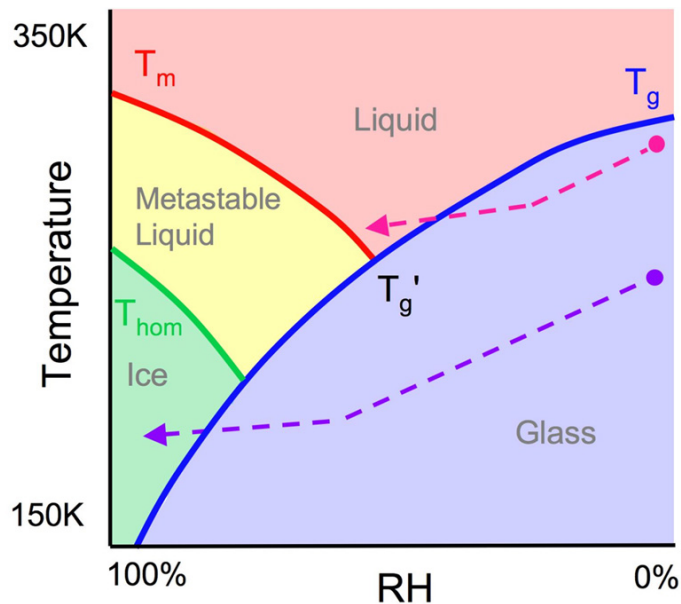


**Fig. 1.** Schematic depicting a generic state diagram for a glass-forming organic compound. Pink and purple arrows represent experimental trajectories followed in this study.  $T_g'$  is defined as the intersection point of the melting curve ( $T_m$ ) and glass transition curve ( $T_g$ ).

[Title Page](#)[Abstract](#)[Introduction](#)[Conclusions](#)[References](#)[Tables](#)[Figures](#)[◀](#)[▶](#)[◀](#)[▶](#)[Back](#)[Close](#)[Full Screen / Esc](#)[Printer-friendly Version](#)[Interactive Discussion](#)

Glassy aerosol and  
ice nucleation

K. J. Baustian et al.

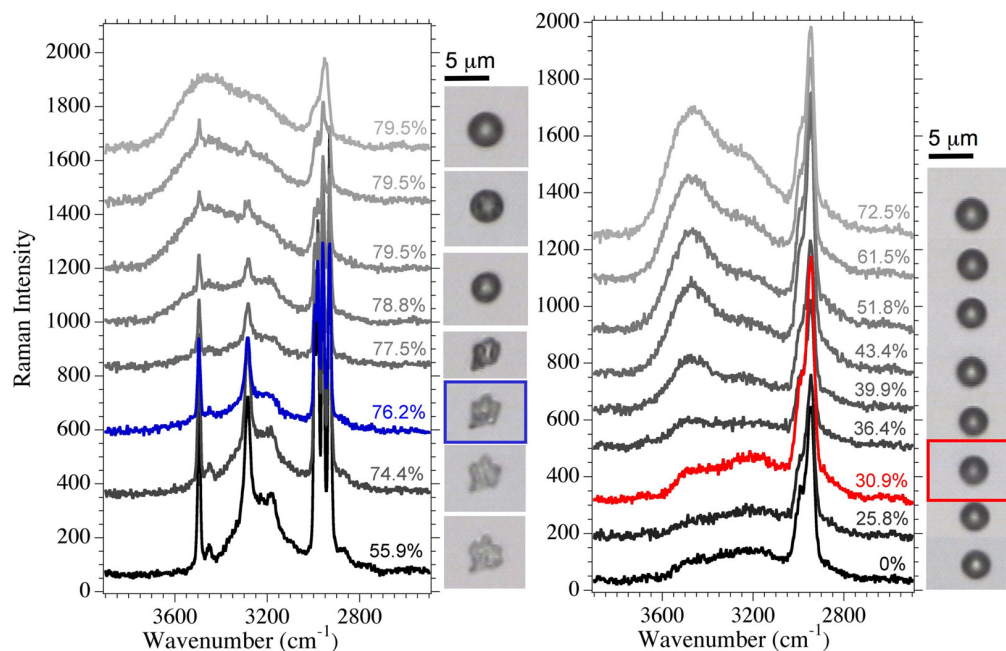


**Fig. 2.** Raman spectra and images demonstrating crystalline (left) and amorphous deliquescence (right) of a citric acid particle at 252 and 257 K, respectively. The onset of water uptake for each experiment was determined using spectral subtraction and indicated by spectra highlighted in blue and red.

[Title Page](#)[Abstract](#)[Introduction](#)[Conclusions](#)[References](#)[Tables](#)[Figures](#)[◀](#)[▶](#)[◀](#)[▶](#)[Back](#)[Close](#)[Full Screen / Esc](#)[Printer-friendly Version](#)[Interactive Discussion](#)

## Glassy aerosol and ice nucleation

K. J. Baustian et al.

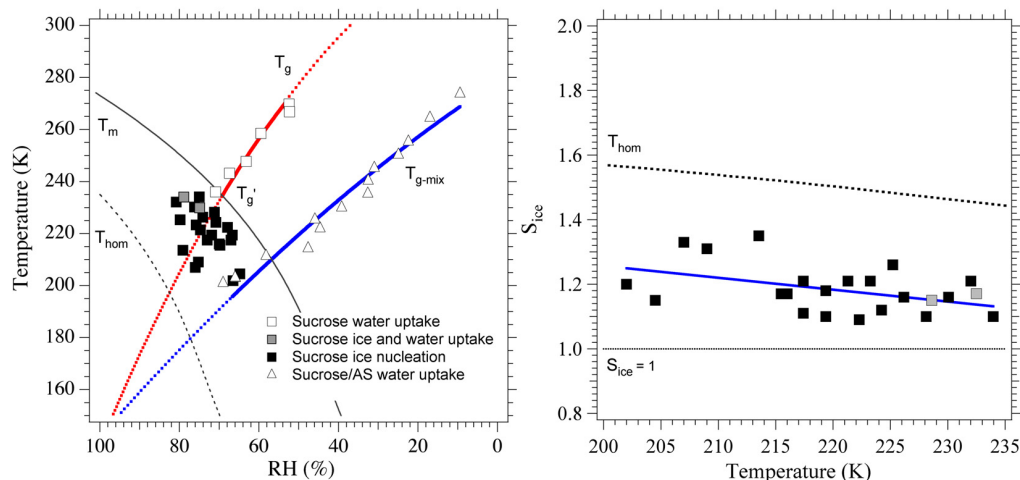


**Fig. 3.** The left panel shows the state diagram for sucrose.  $T_g$  (red) and  $T_{g-mix}$  (blue) lines were created by fitting polynomial curves to experimental water uptake data.  $T_m$  is the melting curve and indicates where  $S_{ice} = 1$ . Black markers represent experiments in which depositional ice nucleation was observed without water uptake. For experiments indicated by gray markers, depositional ice nucleation was observed on one particle while liquid water was simultaneously detected on other particles within the same field of view. The right panel is a plot of ice saturation ratios as a function of temperature for each of the experiments in which ice nucleation was observed.  $T_{hom}$  in both figures indicates where homogeneous ice nucleation would occur in liquid particles according to the parameterization of Koop et al. (2000). Fit parameters for  $T_g(RH)$  curves are given in Table A1.

Title Page

Abstract

Introduction

Conclusions

References

Tables

Figures

◀

▶

◀

▶

Back

Close

Full Screen / Esc

Printer-friendly Version

Interactive Discussion



## Glassy aerosol and ice nucleation

K. J. Baustian et al.

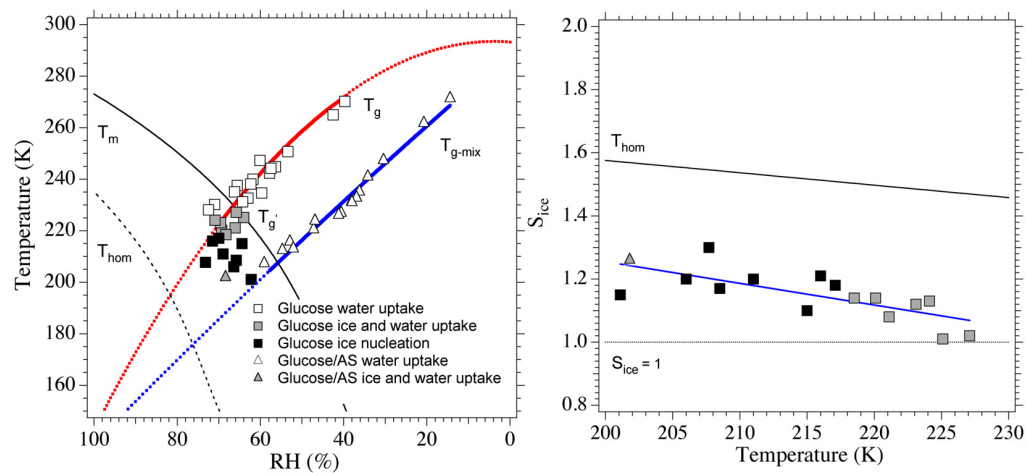


**Fig. 4.** State diagram and corresponding  $S_{ice}$  plot for all experiments in which glucose or glucose/ammonium sulfate was investigated. Other symbols, lines and notation are the same as in Fig. 3.

Title Page

Abstract

Introduction

Conclusions

References

Tables

Figures

◀

▶

◀

▶

Back

Close

Full Screen / Esc

Printer-friendly Version

Interactive Discussion



## Glassy aerosol and ice nucleation

K. J. Baustian et al.

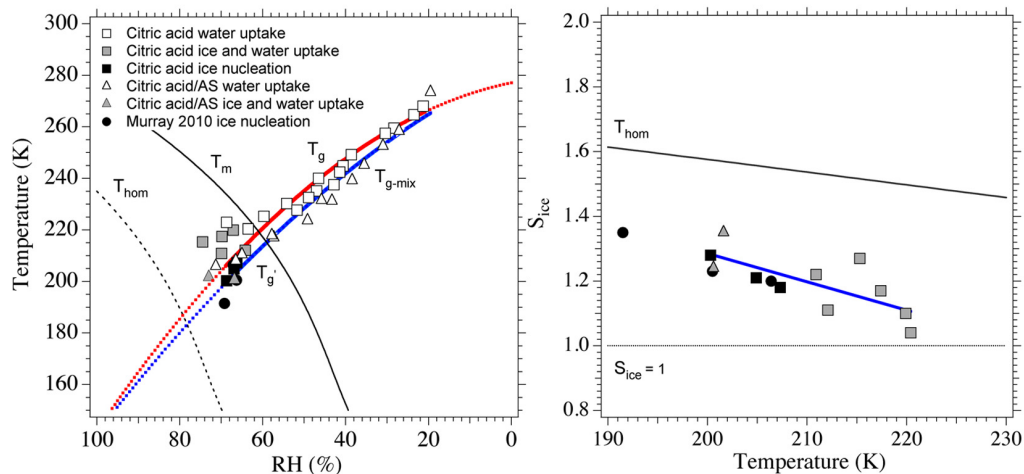


**Fig. 5.** State diagram and plot of ice saturation ratios for all water uptake and ice nucleation experiments performed on citric acid and citric acid/ammonium sulfate particles. Black circles in this figure represent ice nucleation on citric acid as observed during cloud chamber experiments from Murray et al. (2010). Other symbols, lines and notation are the same as in Fig. 3.

[Title Page](#)
[Abstract](#)
[Introduction](#)
[Conclusions](#)
[References](#)
[Tables](#)
[Figures](#)
[◀](#)
[▶](#)
[◀](#)
[▶](#)
[Back](#)
[Close](#)
[Full Screen / Esc](#)
[Printer-friendly Version](#)
[Interactive Discussion](#)


**Glassy aerosol and  
ice nucleation**

K. J. Baustian et al.

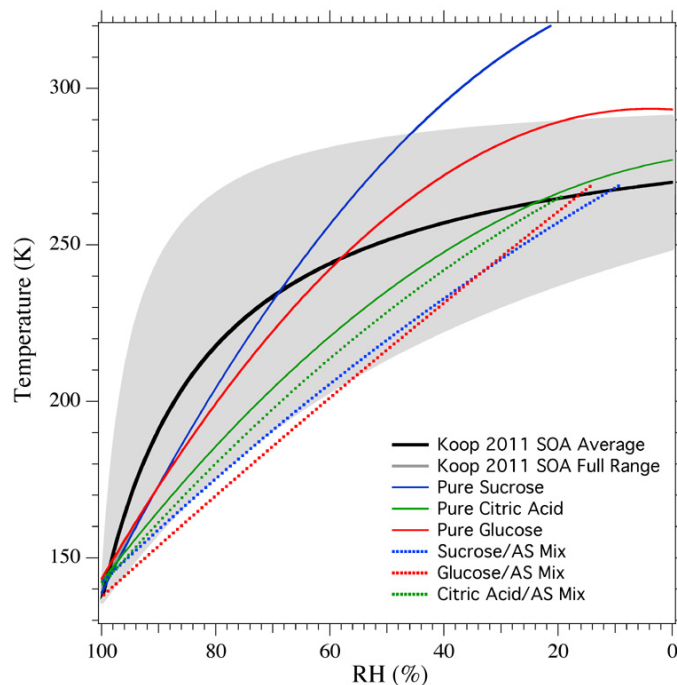


**Fig. 6.**  $T_g$ (RH) diagram depicting experimentally determined glass transition curves from this study and the estimated range for atmospheric SOA particles from Koop et al. (2011). This plot indicates that the organics and mixtures investigated in this study may be good proxies for atmospheric SOA (method adapted from Wilson et al., 2012).

[Title Page](#)[Abstract](#)[Introduction](#)[Conclusions](#)[References](#)[Tables](#)[Figures](#)[◀](#)[▶](#)[◀](#)[▶](#)[Back](#)[Close](#)[Full Screen / Esc](#)[Printer-friendly Version](#)[Interactive Discussion](#)

## Glassy aerosol and ice nucleation

K. J. Baustian et al.

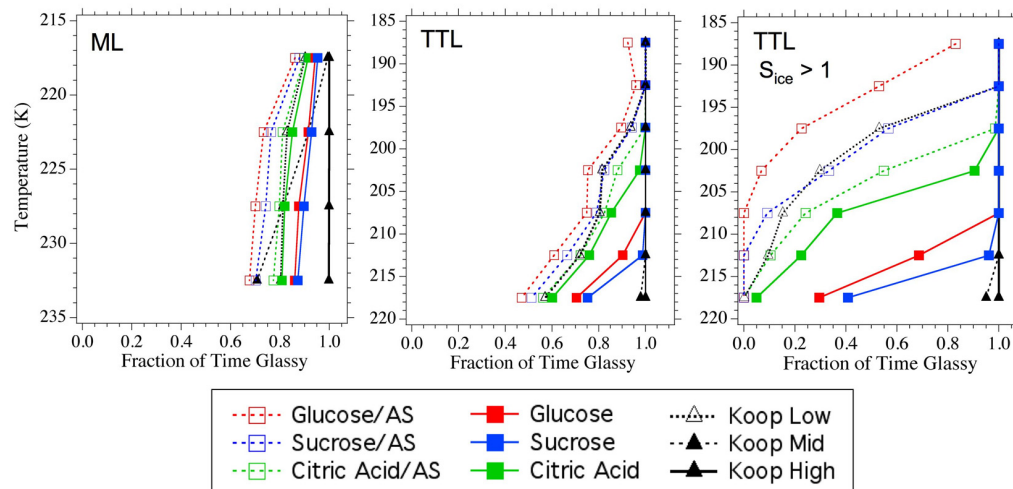


**Fig. 7.** Left and middle panels show the fraction of time organic and mixed organic ammonium sulfate (AS) particles are predicted to be glassy for midlatitude upper troposphere (ML) and TTL conditions. Modeled results for the range of  $T_g$  values predicted for atmospheric SOA by Koop et al. (2011) are also included in black. The right panel shows the fraction of time aerosol of each type will be glassy at TTL conditions for ice nucleation ( $S_{ice} > 1$ ).

Title Page

Abstract

Introduction

Conclusions

References

Tables

Figures

I◀

▶I

◀

▶

Back

Close

Full Screen / Esc

Printer-friendly Version

Interactive Discussion

